Probing asymmetry and self-similarity of fully developed turbulence

Samuel I. Vainshtein
Department of Astronomy and Astrophysics, University of Chicago, Chicago, Illinois 60637
(Received 2 July 1997)

An experimental study of atmospheric turbulent flow has been made to probe self-similarity and deviation from self-similarity of turbulence. Special emphasis is made on asymmetry as an indicator of the deviation from self-similarity. The scaling exponents for positive and negative parts of the velocity increments have been obtained for several moment orders, up to the sixth. The exponents do show asymmetry, predicted by the so-called ramp-model [S. I. Vainshtein and K. R. Sreenivasan, Phys. Rev. Lett. **73**, 3085 (1994)]. This asymmetry, however, can be estimated as moderate. Much more pronounced asymmetry is found in the tails of the velocity increments probability distribution function (PDF's). In particular, the odd moments are mainly defined by the asymmetry of the tails, rather than by that of the PDF core. The deviation from self-similarity is also quite pronounced for the joint two-point PDF. [S1063-651X(97)11212-0]

PACS number(s): 47.27.Ak, 47.27.Jv

I. INTRODUCTION

The similarity hypotheses, suggested by Kolmogorov [1,2], have been studied for a long time. The so-called Kolmogorov 1941 (K41) theory implies self-similar behavior, that is, scaling laws for the structure functions, these functions being introduced in the above-mentioned papers.

The similarity hypotheses is a subject of intense studies, not abating until now, see, e.g., recent review [3]. The reason is that the two similarity hypotheses [1,2] in fact correspond to nonintermittent systems. For Gaussian statistics, of course, there is no intermittency, and the K41 two similarity hypotheses would be confirmed. It is interesting to note that the real distribution cannot be Gaussian *a priori* because of Kolmogorov law, also found in K41 [1]. Indeed, the latter implies that the third moment of the velocity increments does not vanish (and the first does for statistically homogeneous systems), and therefore the distribution is asymmetric, and non-Gaussian.

This asymmetry is known, of course; the probability distribution function, PDE, can be seen to be asymmetric, at least by measuring the skewness (which is known to be negative). The asymmetry of the PDF is not very pronounced at the core, where the velocity increments change within, say, three standard deviations; see, e.g., [4]. That is, say, 99.7% of events (if the PDF core can be approximated as Gaussian distribution) is not really asymmetric. This ''natural'' asymmetry, due to the Kolmogorov law, was traditionally interpreted as a manifestation of turbulent energy cascade to the small scales [5].

It has been suggested recently that the asymmetry may be also related to the deviation from self-similarity, i.e., in fact it is related to the intermittency [6]. And indeed, both experimental measurements in pipe turbulence and direct numerical simulations [7] seem to confirm the so-called ramp model, suggested in [6], see also [4]. These measurements corresponded to the statistics of low moments, or, alternatively, to the PDF core. The aim of this paper is to study the asymmetry related phenomena at higher order statistics, or, equivalently, at the PDF tails, where the intermittency is directly manifested. This may give us more straightforward insight into the relationship between the asymmetry and intermittency of fully developed turbulence.

II. DESCRIPTION OF METHODS AND CONTENTS OF THE PAPER

The main approach used in this paper is experimental. The measurements reported here present data from atmospheric turbulence, obtained at Yale University. A hot-wire anemometer was placed about 35 m above the ground. Mean wind speed was 7.6 m/sec, root-mean-square velocity 1.3 m/sec. Using Taylor's hypothesis and local isotropy assumption to obtain dissipation, one obtains the Taylor microscale Reynolds number to be 9540, and the Kolmogorov microscale η to be 0.57 mm. The data were sampled at 5 kHz, and the whole data set consists of 10×10^6 data points (courtesy of K. R. Sreenivasan).

This data set was divided into four files, each of them consisting of 2.5×10^6 data points. We will refer to them as runs A, B, C, and D. Each run was treated separately, as if we had four separate experiments. This made it possible to study convergence of quantities under consideration. The main results, like calculation of moments of different orders, are eventually averaged over all four files, provided the convergence is satisfactory. Some of the results from different runs are compared with each other. For example, the tails of the PDF present rare events, and it is useful to see the difference and common features from different runs.

The paper mainly deals with statistics of the velocity increments for different separations r. The separation is conventionally given in terms of Kolmogorov length η. We will prefer, however, to use the sample length r_0, corresponding to the smallest separation between two data points in any particular experiment. There are two reasons for that. First, the distributions with $r=r_0$, corresponding to the velocity gradient, play a special role, see, e.g., [4]. In particular, it is straightforward to provide the box counting for integer box sizes, that is, in terms of r_0. Second, we also study in this paper the two-point joint velocity statistics, for which case the Kolmogorov scale does not have an obvious preference. Therefore, in order to keep the units the same throughout the paper, we prefer to plot all distances in units of $r_0=1$. This

 © 1997 The American Physical Society

should not lead to confusion, at least because the Kolmogorov scale has the same order of magnitude as r_0. In fact, $\eta=0.4r_0$, so that we may expect the inertial range to appear at $r>10r_0$, say.

We study self-similar PDF for the velocity increments in Sec. III, with emphasis on the requirements that the self-similarity imposes on the positive and negative velocity increments separately, that is, on the asymmetry of statistics. In Sec. IV, the self-similar joint two-point PDF is introduced. Section V presents experimental evidence of the deviation from the self-similarity for the velocity increments PDF. The section in part compiles previous results, and in addition presents new measurements from the *A*, *B*, *C*, and *D* runs. Special attention is devoted to the asymmetry, where this deviation is manifested more strongly. Section VI describes the measurements of the joint PDF, and its deviation both from Gaussian, and from self-similar form. Finally, the main conclusions are given in Sec. VII.

III. SELF-SIMILAR PDF

We start with the PDF for the velocity increments $u=\Delta_r v=v(x+r)-v(x)$, where $v(x)$ and $v(x+r)$ are longitudinal components of the velocities at points x and $x+r$ correspondingly. Generally, for homogeneous turbulence, the PDF, $p(u|x,x+r)$, is a function of two arguments, $p(u|x,x+r)\equiv P(u,r)$. There is an obvious symmetry for the PDF,

$$P(u,r)=P(-u,-r), \tag{1}$$

or, in a more compact form,

$$P(u,r)=P(nu,r), \quad n=\frac{r}{|r|}. \tag{2}$$

The PDF can be called self-similar, if it obeys the scale transformation formula

$$P(u,\lambda r)du=P(hu,r)dhu, \tag{3}$$

where, generally, the scale function, $h\equiv h(r,\lambda)$. Naturally, $h(r,\lambda=1)=1$. The function $h(r,\lambda)$ can be specified, considering λ in the vicinity of unity, $\lambda=1+\delta$, $\delta\ll 1$. Then, $h(r,\lambda)=1+\delta g(r)$, where $g(r)=\partial_\lambda h(r,\lambda=1)$.

Equation (3) is now reduced to

$$P(u,r)g(r)+\frac{\partial P(u,r)}{\partial u}g(r)u-\frac{\partial P(u,r)}{\partial r}r=0, \tag{4}$$

with the general solution,

$$P(u,r)=\frac{1}{\sigma(r)}\Phi\left(\frac{u}{\sigma(r)}\right), \tag{5}$$

where Φ is an arbitrary function, and

$$\sigma(r)=e^{-\int(g/r)dr}.$$

Substituting Eq. (5) back into Eq. (3), we get for arbitrary λ,

$$h(r,\lambda)=\frac{\sigma(r)}{\sigma(\lambda r)}. \tag{6}$$

It can be seen from Eq. (5) that the PDF can be written as a function of one argument, namely,

$$p\left(\frac{u}{\sigma(r)}\middle| r\right)=\Phi(X), \quad X=\frac{u}{\sigma(r)}, \tag{7}$$

and that is the reason it can be called self-similar.

We define $\sigma(r)$ through the second moment,

$$\sigma(r)^2=\langle u^2\rangle=\int u^2P(u,r)du. \tag{8}$$

For the self-similar PDF,

$$\int \Phi(X)dX=1, \tag{9}$$

(normalization), and

$$\int \Phi(X)X^2dX=1, \tag{10}$$

which follows from definition (8).

As $\sigma(r)^2$ corresponds to a structure function of the second order, it behaves accordingly. That is,

$$\sigma(r)^2=2[K(0)-K(r)], \tag{11}$$

where $K(r)$ is velocity correlation function,

$$K(r)=\langle v(x+r)v(x)\rangle.$$

Therefore, $\sigma(r=0)=0$, and

$$\sigma(r\to\infty)^2\to 2K(0)=2\max\{K(r)\}>0. \tag{12}$$

As the PDF may not be negative, the function $\sigma(r)$ cannot be negative either, see Eq. (5), that is, $\sigma(r)\geqslant 0$, and

$$\sigma(-r)=\sigma(r). \tag{13}$$

So far, apart from restrictions (11)–(13), the function $\sigma(r)$ is arbitrary, and, in particular, it need not be a power law. We can assume, though, that the PDF is self-similar in a narrow sense as well, in addition to the requirement (3). Namely, let

$$\sigma(\lambda r)=h(\lambda)\sigma(r). \tag{14}$$

Considering again $\lambda=1+\delta$, we get

$$\sigma(r)=Cr^p, \quad p=\frac{dh}{d\lambda}(\lambda=1)=\text{const}, \tag{15}$$

an analog of Eq. (5), and $h(\lambda)=\lambda^p$, an analog of Eq. (6). However, there is no need for assumption (14), as shown below.

Returning to the general requirement (1), we see that the self-similar PDF must satisfy $\Phi(-X)=\Phi(X)$ to be an even

function. Real PDF is asymmetric, and therefore, we have to relax the requirement (3) and write the PDF in a more general form,

$$P(u,r)=\frac{1}{\sigma(r)}\,\Phi\left(\frac{nu}{\sigma(r)}\right), \tag{16}$$

Thus, $\Phi=\Phi(nX)$ is a function of two arguments, and hence, strictly speaking, the PDF is not self-similar. However, the r dependence enters only through the sign of r, and therefore we will still refer to the PDF in the form (16) as self-similar.

We now calculate the structure functions, $\widetilde{S}_m(r)=\langle u^m\rangle$, where m is an integer, and generalized structure functions, $S_q(r)=\langle|u|^q\rangle$ (q is arbitrary). It follows from Eq. (16) that

$$\widetilde{S}_m(r)=\widetilde{s}(m)\sigma(r)^m, \tag{17}$$

where

$$\widetilde{s}(m)=\int\Phi(nX)X^n dX$$

and

$$S_q(r)=s(q)\sigma(r)^q, \tag{18}$$

where

$$s(q)=\int\Phi(X)|X|^q dX.$$

It is clear, first, that, for even m, $\widetilde{S}_m(r)=S_m(r)$. Second, $\widetilde{s}(0)=s(0)=1$, from Eq. (9); $\widetilde{s}(1)=0$ (follows from homogeneity, $\langle u\rangle=0$); and finally $\widetilde{s}(2)=s(2)=1$, by definition (10).

If the PDF would be symmetric, then all the structure functions of odd orders vanish, $\widetilde{s}(m=2l+1)=0$, l is integer. However, the third moment does not vanish. As a matter of fact, according to the Kolmogorov law [1], in inertial range,

$$\widetilde{S}_3(r)=-\tfrac{4}{5}\epsilon r, \tag{19}$$

where ϵ is the energy dissipation rate.

Therefore,

$$\widetilde{s}(3)\sigma(r)^3=-\tfrac{4}{5}\epsilon r,$$

so that

$$\sigma(r)\sim r^{1/3}.$$

Specifying the coefficient, we have

$$\sigma(r)=C_2^{1/2}(\epsilon r)^{1/3}. \tag{20}$$

Here the coefficient C_2 is chosen in such a way that Eq. (11) is satisfied. Thus, the power law for $\sigma(r)$ follows from the general self-similarity requirement (3) and the Kolmogorov law: no need to assume the self-similarity in a narrow sense, as in Eqs. (14) and (15).

It then follows from Eqs. (17) and (18) that

$$\widetilde{S}_m(r)=\widetilde{s}(m)(C_2^{3/2}\epsilon r)^{m/3}\sim r^{\xi m},\quad \xi_m=\frac{m}{3}, \tag{21}$$

and

$$S_q(r)=s(q)(C_2^{3/2}\epsilon r)^{q/3}\sim r^{\zeta_q},\quad \zeta_q=\frac{q}{3}. \tag{22}$$

Obviously, for the self-similar PDF, $\xi_m=\zeta_m$, and, in particular,

$$\zeta_3=\xi_3=1. \tag{23}$$

Thus, the PDF in the form (16), plus the Kolmogorov law (19), recover the K41 hypotheses. On the other hand, the PDF is defined if all moments are known [5], and therefore the form (16) is unambiguously defined by the K41 hypotheses [4], see also [8].

It follows from Eq. (17) that skewness

$$S_k(r)=\frac{\widetilde{S}_3(r)}{\widetilde{S}_2(r)^{3/2}}=\widetilde{s}(3)=\text{const}, \tag{24}$$

and flatness

$$F_4(r)=\frac{S_4(r)}{S_2(r)^2}=s(4)=\text{const}. \tag{25}$$

It is noteworthy that the PDF in general self-similar form (16) cannot be valid everywhere for arbitrary r. Indeed, any odd moment of the structure function must vanish at $r\to\infty$, or, to be more specific, it should be small at $r\gg l$, where l is the integral (or correlation) length. However, according to Eq. (17) and Eqs. (11) and (12), the structure function asymptotically approaches a constant. That means that the most general self-similar PDF should be written in the form

$$P(u,r)=\frac{1}{\sigma(r)}\,\Phi\left(\frac{nu}{\sigma(r)},r\right), \tag{26}$$

where the explicit r dependence in Φ is negligible for $r\ll l$, and for $r\gtrsim l$ the PDF becomes symmetric (so that the odd moments vanish). As the inertial range is defined as $\eta\ll r\ll l$, where η is the Kolmogorov scale, the PDF in the form (16) can be accepted for small and moderate r. At $r\gg l$, the PDF is automatically independent of r (presenting statistics of the sum of two independent variables), and therefore Eq. (16) can be used again: this time, with symmetric Φ. Only at $r\approx l$ does the presentation (16) fail, and the PDF should be written in general form (26).

As the goal of this paper is to study the deviation from self-similarity, we note that asymmetry is quite a sensitive indicator of this deviation. In order to see that, we will consider, following [6], the positive and negative moments separately. That is, denote $S_q^+(r)$ the structure functions for positive increments, and $S_q^-(r)$ for negative. In other words,

$$S_q^+(r)=\int_0^\infty u^q p(u|r)du,\quad S_q^-(r)=\int_{-\infty}^0|u|^q p(u|r)du,$$

so that

$$S_q(r)=S_q^+(r)+S_q^-(r),\quad \widetilde{S}_m(r)=S_m^+(r)-S_m^-(r).$$

For the PDF in the form (16), if valid,

$$S_q^+(r)=s_q^+\sigma(r)^q, \quad S_q^-(r)=s_q^-\sigma(r)^q, \tag{27}$$

where

$$s_q^+=\int_0^\infty \Phi(nX)X^q dX, \quad s_q^-=\int_{-\infty}^0 \Phi(nX)|X|^q dX.$$

IV. SELF-SIMILAR JOINT TWO-POINT PDF

Consider the two-point PDF, $p(v,v'|x,x')=P(v,v',r)$, $x'=x+r$, the probability density for the velocity to assume the values v and v' at the points x and x'. Note, first, that the PDF obviously obeys the symmetry property,

$$p(v,v'|r)=p(v',v|-r), \tag{28}$$

corresponding to Eq. (1), and, second, the velocity increments PDF used in the previous section follows from the two-point PDF,

$$p(u|r)=\int p(v'-u,v'|r)dv'.$$

It is clear from this expression, and from Eq. (28), that the joint PDF cannot be expected to be self-similar in respect to variables v and v': if it can be written in a self-similar form, then at least one of the variables should be $u=v'-v$. In order to find the second variable, we first define two-dimensional self-similarity for (unknown) variables $\tilde{v}$ and $\tilde{v}'$, both presenting some combinations of the velocities v and v'. Namely, the PDF is self-similar if it obeys

$$P(\tilde{v},\tilde{v}',\lambda r)d\tilde{v}d\tilde{v}'=P(h\tilde{v},h'\tilde{v}',r)dh\tilde{v}dh'\tilde{v}', \tag{29}$$

where $h\equiv h(r,\lambda)$, and $h'\equiv h'(r,\lambda)$, cf. Eq. (3). Considering again the scale factor λ in the vicinity of unity, $\lambda=1+\delta$, we obtain the following equation for P,

$$Pg(r)+\frac{\partial P}{\partial \tilde{v}}g(r)\tilde{v}+\frac{\partial P}{\partial \tilde{v}'}g'(r)\tilde{v}'-\frac{\partial P}{\partial r}r=0, \tag{30}$$

where $g(r)=\partial_{\tilde{v}}h(r,\lambda=1)$, and $g'(r)=\partial_{\tilde{v}'}h'(r,\lambda=1)$, with the general solution

$$P=\frac{1}{\tilde{\sigma}(r)\tilde{\sigma}'(r)}\Phi\left(\frac{\tilde{v}}{\tilde{\sigma}(r)},\frac{\tilde{v}'}{\tilde{\sigma}'(r)}\right), \tag{31}$$

where

$$\tilde{\sigma}(r)=e^{-\int(g/r)dr}, \quad \tilde{\sigma}'(r)=e^{-\int(g'/r)dr}.$$

As a result, analogous to Eq. (6), we have

$$h(r,\lambda)=\frac{\tilde{\sigma}(r)}{\tilde{\sigma}(\lambda r)} \quad \text{and} \quad h'(r,\lambda)=\frac{\tilde{\sigma}'(r)}{\tilde{\sigma}'(\lambda r)}.$$

It is clear now that if the joint PDF is self-similar, then it can be written as a function of two arguments (instead of three: v, v', and r). Namely,

$$p\left(\frac{\tilde{v}}{\tilde{\sigma}(r)},\frac{\tilde{v}'}{\tilde{\sigma}'(r)}\middle| r\right)=\Phi(X,Y), \quad X=\frac{\tilde{v}}{\tilde{\sigma}(r)}, \quad Y=\frac{\tilde{v}'}{\tilde{\sigma}'(r)}, \tag{32}$$

cf. Eq. (7). As mentioned, one of the variables should be u. Now, in order to keep the symmetry (28), we suggest that the second variable is $v'+v$, so that two ''canonical'' variables read

$$X=\frac{u=v'-v}{\sigma(r)=\langle u^2\rangle^{1/2}}, \tag{33a}$$

$$Y=\frac{u'=v'+v}{\sigma'(r)=\langle u'^2\rangle^{1/2}}, \tag{33b}$$

And indeed, as an example, the Gaussian distribution,

$$p_G(v,v'|x,x')$$
$$=\frac{1}{2\pi[K(0)^2-K(r)^2]^{1/2}}$$
$$\times\exp\left\{-\frac{K(0)v^2-2K(r)vv'+K(0)v'^2}{2[K(0)^2-K(r)^2]}\right\},$$

can be written in a self-similar form,

$$p_G(X,Y)=\frac{1}{2\pi}e^{-(X^2+Y^2)/2}. \tag{34}$$

Here $\sigma(r)$ is found from Eq. (11), as before, and

$$\sigma'(r)^2=\langle u'^2\rangle=\langle(v'+v)^2\rangle=2[K(0)+K(r)]. \tag{35}$$

In addition to being self-similar [the PDF (34) is independent of r], the Gaussian distribution presents two statistically independent variables, X and Y. Besides, the functional dependence of the PDF on the variable X coincides with that for the variable Y. That is to say that there is only one functional dependence in Eq. (34). In general, however, as seen from Eq. (32), the PDF is two dimensional, and cannot be presented as a product $\Phi_1(X)\Phi_2(Y)$, in which case the variables would be independent.

A more general form of self-similar two-point PDF incorporates possible asymmetry, analogous to Eq. (16), that is,

$$p(v,v'|r)=\frac{1}{\sigma(r)\sigma'(r)}\Phi(nX,Y), \tag{36}$$

where X and Y are defined in Eq. (33), or

$$p(X,Y|r)=\Phi(nX,Y), \tag{37}$$

cf. Eq. (7).

We note finally that any joint PDF can be written in terms of dimensionless variables, X and Y, and generally,

$$p(X,Y|r)=\Phi(X,Y,r). \tag{38}$$

The PDF in dimensionless form (38) is useful to measure experimentally, because it can be easily compared with a Gaussian, and with self-similar PDF: in the latter case the PDF should be independent of r.

Obviously,

$$p(X|r)=\int\Phi(X,Y,r)dY, \tag{39}$$

and

$$p(Y|r)=\int \Phi(X,Y,r)dX. \tag{40}$$

V. DEVIATIONS FROM SELF-SIMILARITY

Probing the K41 hypotheses, or, equivalently, the self-similarity of PDF by direct measurements, showed that there are noticeable deviations from K41. Measurements of the scaling exponents of the structure functions showed deviation from K41, that is, there are so-called intermittency corrections to the exponents, given in Eqs. (21) and (22) [9]. In addition, direct measurements of the velocity increments PDF also revealed deviation from the self-similarity. This can be seen from stretched-exponential presentation of the PDF at the tails [10],

$$p(u|r)\sim \frac{1}{\sigma(r)}\exp\{-x^{m(r)}\}. \tag{41}$$

It is the functional dependence $m(r)$ that makes it different from the self-similar form (16). As a matter of fact, this r dependence reflects the well-known fact that the tails are more pronounced for small distances r [11]. The central part of the PDF is not self-similar either [4].

As long as the PDF deviates from the self-similar form, then, strictly speaking, the K41 hypotheses become invalid. Even the mere existence of scaling (21), (22) with exponents, not necessarily coinciding with $\xi_m=m/3$, and $\zeta_q=q/3$, becomes an assumption (namely, that the self-similarity in a narrow sense, Eqs. (14) and (15), holds for structure functions of arbitrary orders). The only scaling that always remains valid is the Kolmogorov law,

$$\xi_3=1, \tag{42}$$

and, in particular, there is no ground *a priori* to state that ζ_3 should be also unity, cf. Eq. (23), although its experimental value *is* quite close to unity.

This kind of deviation is mainly manifested in the tails, or for relatively high moments. That is to say that statistics of rare events are not self-similar. The main events, corresponding to the PDF core, and to the low moments, deviate from Gaussian form, or generally, from the self-similar presentation, but not dramatic. Typically, the deviation is about 10–15% [4].

A. Asymmetry of the moments

It turns out that the asymmetry is much more sensitive to the deviation from self-similarity. Indeed, expression (27) proves to be quite a strong restriction imposed on the PDF. First of all, by Eq. (27), the ratio, $S_m^+(r)/S_m^-(r)=s_q^+/s_q^-=\text{const}$. But, as was already noticed in [7], the experimental measurements of these quantities (for different q) showed that these are not at all constants, see also [4].

Besides, for the zeroth order, $S_0^+(r)=s_0^+=\text{const}$, and $S_0^-(r)=s_0^-=\text{const}$, that is, these two structure functions should be independent of r. Experimental curves, however, are not at all constants, see Fig. 2 in [4]. Moreover, if $S_0^\pm(r)$ would be constant, then these two constants are expected to be $=1/2$. Indeed, at asymptotically large r's, when the PDF becomes symmetric (see the end of Sec. III), these functions should be $=1/2$. Therefore, it is sufficient to calculate $S_0^\pm(r=r_0)$ to check if these quantities are equal to 1/2. It turns out, as an example for the run A, that $S_0^+(r=r_0)=0.444$, and $S_0^-(r=r_0)=0.398$. These values are appreciably less than 1/2, and different from each other. As the $S_0^\pm(r)$ functions should nevertheless asymptotically approach 1/2, they inevitably are functions of r.

In addition to that, the behavior of these functions corresponds to what the ramp-model [6] predicted. Indeed, according to it, the length of the positive part of the signal should be bigger than that of the negative—for all distances. Only at $r\to\infty$ these lengths become equal to 1/2. In other words,

$$S_0^-(r)<S_0^+(r),\quad S_0^\pm(r)\to\tfrac{1}{2}\quad \text{as } r\to\infty, \tag{43}$$

and experimental curves indeed behave accordingly [4].

It has been long observed that flatness $F_4(r)$ is not a constant, as it should be if the PDF is self-similar, see Eq. (25), and the deviation from a constant is supposed to manifest the intermittency. The same should be true for the positive and negative parts of the flatness. Namely, according to Eq. (27), if the PDF is self-similar, then

$$F_4^+(r)=\frac{s_4^+}{(s_2^+)^2},\quad F_4^-(r)=\frac{s_4^-}{(s_2^-)^2}, \tag{44}$$

so that both $F_4^+(r)$ and $F_4^-(r)$ are constants (independent of r). Direct measurements of these quantities (compiled from all four runs) show, however, quite substantial deviation from a constant, Fig. 1(a). Note that the process is quite intermittent. The classical flatness factor, $F_4(r_0)=31.63$ (cf. with Gaussian value 3), asymmetric flatness, $F_4^+(r_0)=55.71$, and $F_4^-(r_0)=68.55$: to compare with Gaussian 6, see [4].

An even more noticeable discrepancy arises from the observation that, if Eq. (16) is valid, then the scaling for $S_q^+(r)$ and for $S_q^-(r)$ should be as good as for the generalized structure function $S_q(r)$: the difference is only in coefficients. In particular, the odd moments for the structure functions should exhibit the same kind of scaling as corresponding moments for the generalized structure functions (except for the first moment, in which case the coefficient $\tilde{s}_1$ turns to zero). However, it was long observed that it is not the case. For example, the generalized structure function $S_3(r)$ normally exhibits bigger inertial (or scaling) range, than the structure function $\tilde{S}_3(r)$, that is the Kolmogorov law. Besides, the inertial range is bigger, and the data scattering is less for the second moment, $S_2(r)=\tilde{S}_2(r)$, than for the Kolmogorov law, see, e.g., [7]. The scaling of the higher odd moments only deteriorates, and, for example, the fifth order structure function is substantially worse in scaling than the fifth order generalized structure function: this can be seen from all four runs, A, B, C, and D, and actually it was observed before.

We present here additional evidence for this observation. Direct measurements of the positive and negative moments of orders $q=1/2$, 1, 2, 3, 4, 5, and 6 show that convergence

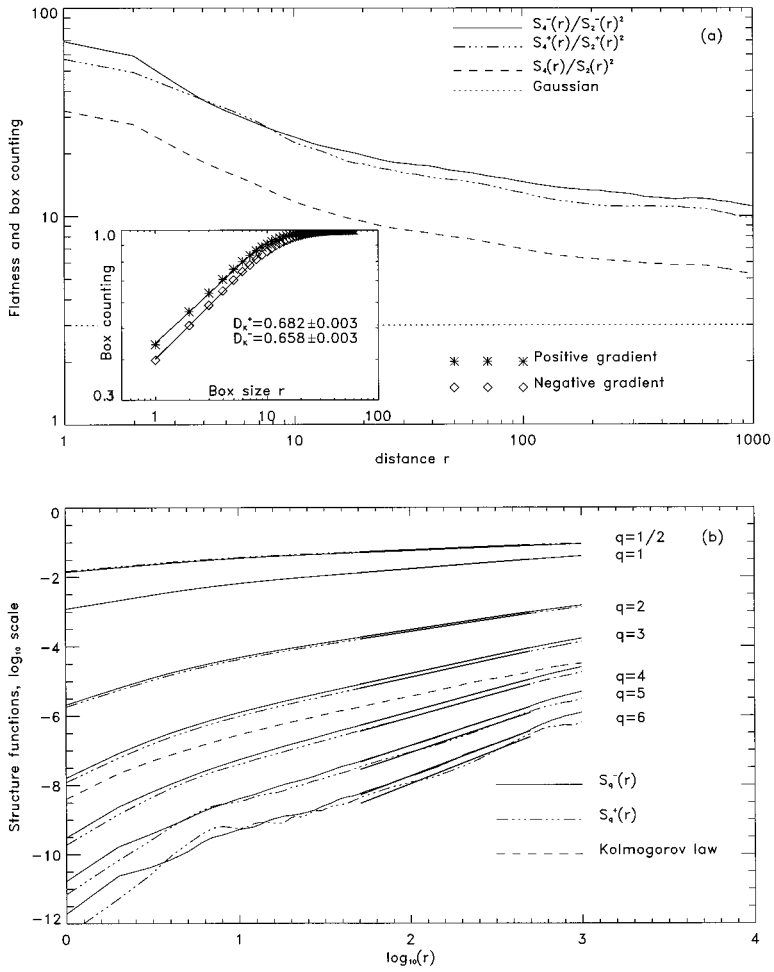

FIG. 1. (a) Flatness for both positive and negative distributions, compared with regular flatness, $S_4(r)/S_2(r)^2$. The inset shows the box counting for the run *A*. The Kolmogorov capacities are different for positive and negative distributions, and $D_K^- < D_K^+$. (b) Structure functions for positive and negative velocity increments. For illustrative purposes the curves are shifted along the ordinate, so that the units are arbitrary. This shifting did not affect, however, the relative distances between the moments of the same order, so that, e.g., the relative positions of $S_3^+(r)$, $S_3^-(r)$, and $\widetilde{S}_3(r)$ are displayed correctly. The distance r is given in units of r_0, see Sec. II. These units are used in all other figures as well.

of the moments is satisfactory only up to the fourth moment. The moments substantially differ for each 2.5×10^6 point run, starting from the fifth order. Recall that the generalized structure functions exhibit good convergence up to the sixth order [12].

Figure 1(b) shows the structure functions listed above; they are compiled from all four runs, that is, from 10×10^6 points. It can be seen that the fifth and sixth moments indeed do not show decent scaling. All this behavior can be understood if we conjecture that *the asymmetry is manifested mainly in the tails of the PDF*. Indeed, the tails represent rare events, and therefore they strongly fluctuate, being different for different realizations. We will seek for substantiation of this hypothesis below. But first we note that Fig. 1(b) mainly confirms the trends found in [7]. Namely, $S^-_{q<1}(r) < S^+_{q<1}(r)$, and $S^-_{q>1}(r) > S^+_{q>1}(r)$, except for few experimental distances for $q=5,6$. However, as mentioned, these two moments show poor convergence anyway, and, for some realizations (with 2.5×10^6 points), $S^-_{5,6}(r) > S^+_{5,6}(r)$ everywhere.

Note that the conjecture mentioned above, relating the asymmetry to the tails, in fact goes back to the ramp model [6], linking the asymmetry with intermittency. A quantitative description of this hypothesis was given by inequality

$$D_q^- < D_q^+, \tag{45}$$

suggesting that at least the generalized dimensions corresponding to the negative distribution, D_q^-, are not trivial. However, because of poor convergence of intermediate moments of positive and negative velocity increments—let alone the higher moments—this inequality was confirmed only for the low moments [7]. Probably, the most trustworthy calculations correspond to $q=0$, that is, to the Kolmogorov capacities [4]. Recall that the generalized dimensions in Eq. (45) are defined by

$$S_q^+(r) \sim r^{(1-\kappa)q-(D-D_q^+)(q-1)},$$

$$S_q^-(r) \sim r^{(1-\kappa)q-(D-D_q^-)(q-1)}, \tag{46}$$

see [6], where D is the dimension of space; we take $D=1$ below, considering a one-dimensional cut of the process. Note, however, that the Kolmogorov capacities are deter-

TABLE I. Asymmetry exponents for different moments q. The corresponding range is chosen as $51 \geqslant r \geqslant 501$, that is one decade. The third moment structure function, i.e., the Kolmogorov law is given on a separate line.

q	S_q^-	S_q^+
1/2	0.195 ± 0.001 (± 0.000)	0.194 ± 0.001 (± 0.000)
1	0.382 ± 0.001 (± 0.000)	0.382 ± 0.001 (± 0.000)
2	0.731 ± 0.003 (± 0.001)	0.737 ± 0.002 (± 0.001)
3	1.047 ± 0.003 (± 0.001)	1.062 ± 0.002 (± 0.000)
	Kolmogorov law 0.990 ± 0.009 (± 0.002)	
4	1.332 ± 0.004 (± 0.001)	1.361 ± 0.005 (± 0.001)
5	1.596 ± 0.004 (± 0.002)	1.643 ± 0.017 (± 0.006)
6	1.847 ± 0.005 (± 0.003)	1.922 ± 0.044 (± 0.013)

mined in [4] directly from the box counting, and according to the definition given by Kolmogorov. Recall that the scaling for the box counting is given by expressions

$$B_0^{\pm}(r|r_0) \sim r^{D-D_K^{\pm}},$$

[cf. Eq. (46) for $q=0$], where $B_0^{\pm}(r|r_0)$ is the box counting for two distributions, $u^{\pm}=[|u(r_0)| \pm u(r_0)]/2$ (corresponding in fact to the velocity gradient, the positive and negative parts being treated separately), and r being the box size. An example of such a counting is also given in the inset to Fig. 1(a), from the run A. The difference between D_K^+ and D_K^- is certainly within confidence level. Note that the expression (46), relating the structure function exponents to the generalized dimensions without invoking the refined Kolmogorov hypotheses [13], was obtained in [14].

In spite of poor convergence of the fifth and sixth moments, we attempted to find a scaling range for all measured moments, and to fit the curves with power laws. This range proved to be for one decade [bold straight lines on Fig. 1(b)]. Table I shows the exponents found this way. The error bars correspond to standard deviation (from the straight line fits), and in the parentheses the errors are defined from usual routines, treating the data scattering as Gaussian noise. It can be seen that the Gaussian errors are always smaller than standard deviation, and so we accept the conservative estimation of the errors in all calculations below: in particular, for the generalized dimensions estimations, see Fig. 2. It is clear

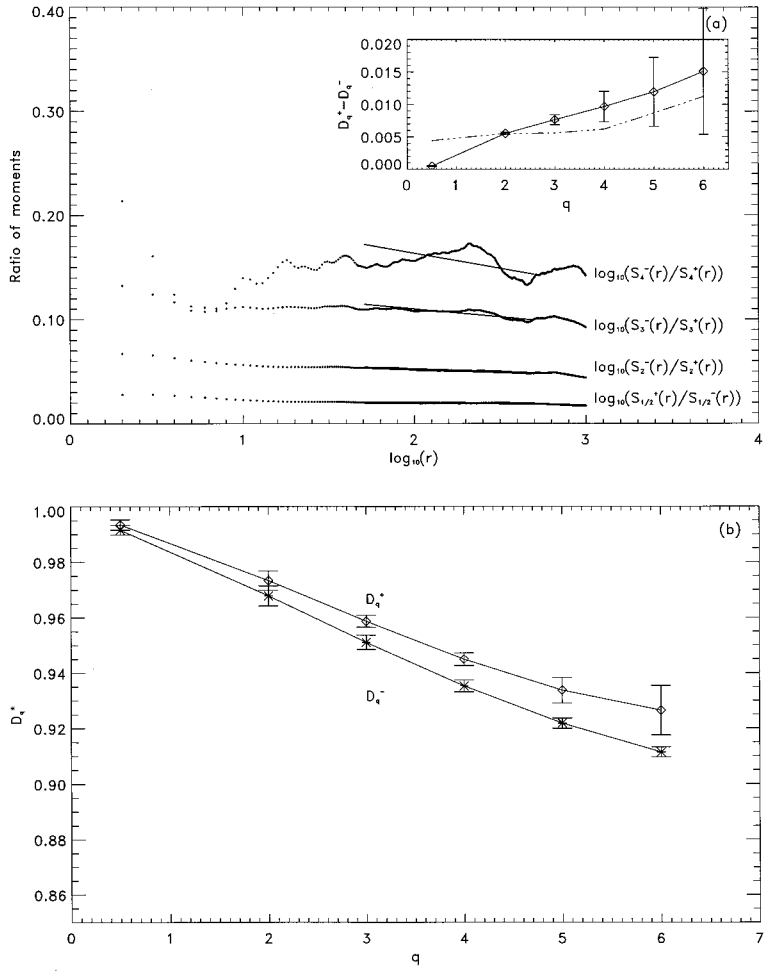

FIG. 2. (a) The ratios of negative and positive moments, $S_q^-(r)/S_q^+(r)$, for $q>1$, inverse ratio $S_q^+(r)/S_q^-(r)$ for $q=1/2$, and fitting in logarithmic scale. The inset gives the difference between the generalized dimensions. The solid line corresponds to the differences calculated directly from the ratios, and the dash-dotted line corresponds to these differences derived from the structure functions for $r=r_0$. (b) The generalized dimensions for positive and negative distributions, calculated from Eq. (46).

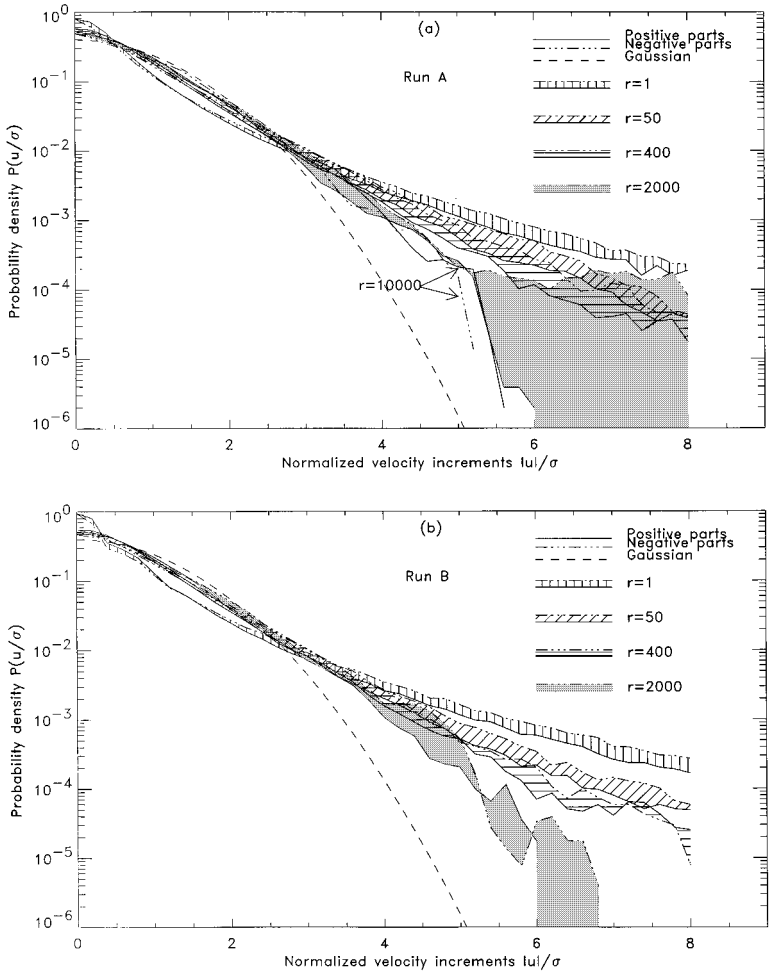

FIG. 3. Asymmetry of the PDF for two runs: (a) run A, and (b) run B. The positive and negative parts of the PDF are plotted in such a way that they can be easily compared. The negative tails are always above the positive ones for small and moderate distances, say up to $r=1000$. This could be true even for $r=2000$, as seen from the run A. Normally, however, this excess disappears at big r's, together with the disappearance of the tails themselves.

from the estimation of the third moment, that is, the Kolmogorov law, that conservative error bars indeed correspond to the law (42), and the Gaussian errors can be considered as an underestimation.

It can be seen that the errors do become big for high moments. However, the differences between the positive and negative distributions exponents are always within the confidence level. This difference corresponds to the difference in the generalized dimensions, as seen from Eq. (46). As the difference is the main issue here, we tried to find an independent way to its estimation, and that is by directly fitting the ratio of the negative and positive moments plotted on Fig. 2(a). The scaling range coincides with that in Fig. 1(b). We can see that, first, the ratio is never a constant, being rather a function of distance; as mentioned, this is also true for the pipe experiments, see [7], and [4], and the beginning of this subsection. Second, although the fitting for the moments ratios for $q \geqslant 4$ do not look nice, the differences between the generalized dimensions are still inside the confidence level, that is, statistically significant; see inset to this figure. These differences are consistent with direct estimation of the dimensions, depicted on Fig. 2(b). It can be seen from the figure that, in spite of substantial data scattering, the differences between the exponents obey Eq. (45), although the numerical values of these differences are small; see Table I. Also, we see from both spectra D_q^+ and D_q^- that they decrease monotonously with q as should be according to the theorem [15]. This gives additional credit to the exponents given in Table I. Indeed, due to substantial scattering of the curves for the high moments, the corresponding exponents could have been simply spurious, and would not necessarily obey the theorem.

One more independent way to measure the differences between the generalized dimensions is to make use of Eq. (46) at $r=r_0$. This corresponds to studying the velocity gradient asymmetry. Or, in other words, using Eq. (46), we have

$$\frac{\langle (u^-)^q \rangle}{\langle (u^+)^q \rangle} = \frac{S_q^-(r_0)}{S_q^+(r_0)} = A\left(\frac{r_0}{l}\right)^{(D_q^- - D_q^+)(q-1)},$$

where a constant A can be determined from the experimental curve for $q=1$. The experimental value is very close to unity (which is quite natural). Another constant r_0/l cannot be found *a priori*, and therefore this formula gives only the sign of the difference $D_q^+ - D_q^-$, and the trend. The difference proves to be positive indeed, as expected from Eq. (45), and increasing with q: see the inset to Fig. 2(a). The correspond-

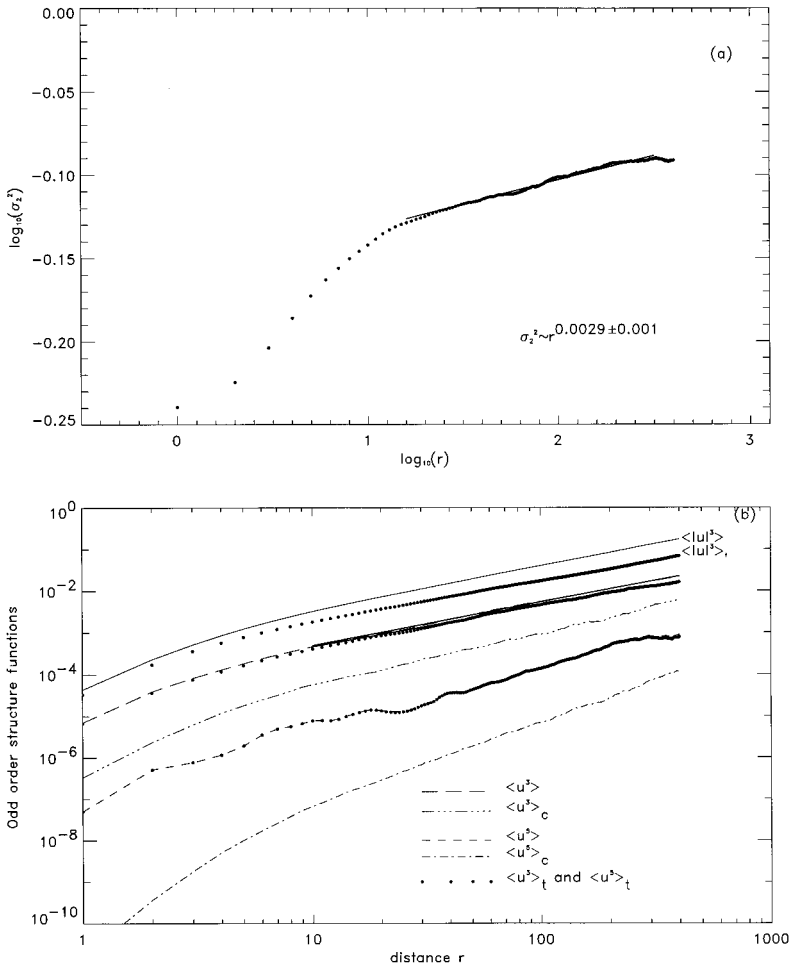

FIG. 4. Contribution of the tails into the structure functions. (a) The r dependence of $\sigma_2(r)$, that is, the effective width of the PDF core, or, to be more exact, the ratio of the second order cumulative structure function $\langle u^2 \rangle_c$ to the structure function $\langle u^2 \rangle$. (b) Comparison of the Kolmogorov law, i.e., the third order structure function, $\langle u^3 \rangle$, the third order generalized structure function, $\langle |u|^3 \rangle$, and the fifth order structure function, $\langle u^5 \rangle$, with the cumulative structure functions, $\langle u^3 \rangle_c$, $\langle |u|^3 \rangle_c$, $\langle u^5 \rangle_c$, and with the contribution of the tails, $\langle u^3 \rangle_t$, $\langle |u|^3 \rangle_t$, and $\langle u^5 \rangle_t$.

ing (dash-dotted) curve is adjusted in such a way that the differences obtained in two different ways coincide at $q = 2$. This procedure defines the unknown constant r_0/l. Although one cannot claim perfect agreement between the solid and dash-dotted lines on the figure, but still, the difference is positive for both of them, and the trend is to increase with growing q.

B. Asymmetry of the PDF

The velocity increments PDF is known to be asymmetric, and that can be seen from many plots, see, e.g., [11]. In order to check the conjecture that asymmetry is manifested in the tails, we compare the positive and negative tails directly. Figure 3 depicts positive and negative parts of the PDF for two files: run A in Fig. 3(a) and run B in Fig. 3(b).

We note first that the deviation of the PDF from the self-similar form (16) is very pronounced: it definitely does not look like the same function for different r's. The tails are substantially bigger for small distances (cf. with [4] where it was shown that the central part also changes with r, but only on, say, 10%–15%). This is, however, a well-known observation, see, e.g., [11], and formula (41) above.

In addition, this figure shows the asymmetry in the tails. Indeed, the negative parts are systematically higher than the positive ones. This means that negative parts are always more intermittent than the positive, in accordance with formula (45). This picture actually repeats itself for different runs; however, the big distances behave peculiarly. It can be seen from Fig. 3(a) that, for run A, the asymmetry for $r = 2000$ proves to be gigantic: there were no events with $u > 6\sigma_{r=2000}$, and a relatively big number of events with $u < -6\sigma_{r=2000}$ were observed. This is an anomaly, however, as seen from run B (although there were no events with $u > 6\sigma_{r=2000}$ either). Other runs also show that the asymmetry for this distance is ''normal,'' i.e., as in run B. The asymmetry practically disappears for very big distances, and the PDF approaches the Gaussian curve: that is, the tails disappear as well.

To probe further the contribution of the tails, we define, following [16], cumulative structure functions,

$$\langle u^m \rangle_c = \int_{-cr}^{cr} u^m p(u|r) du,$$

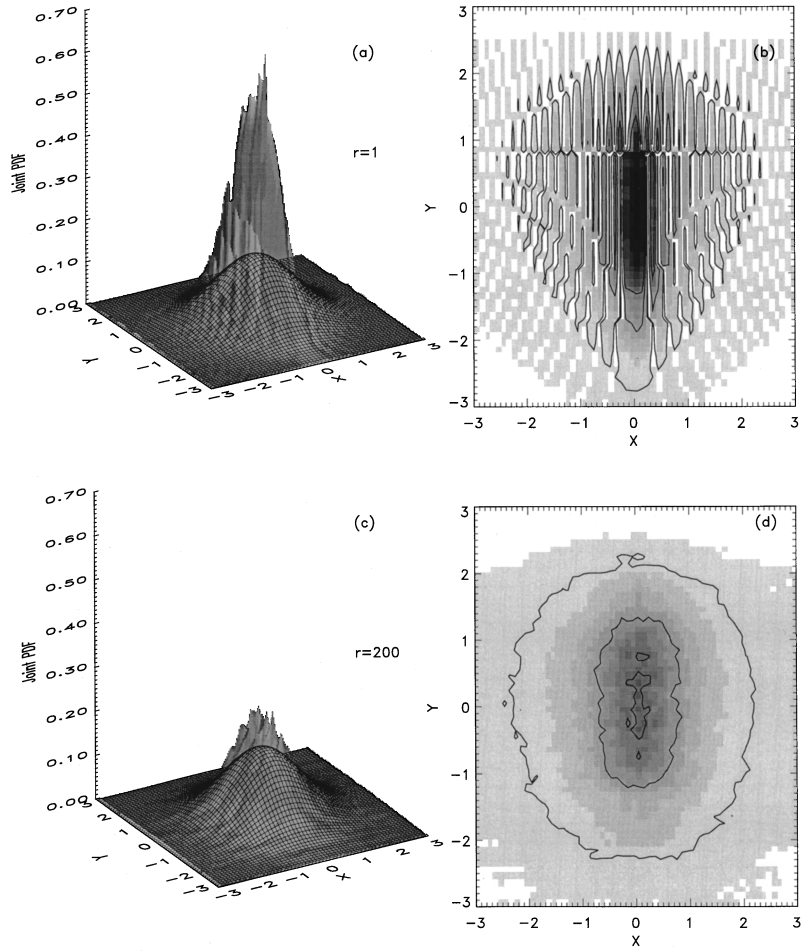

FIG. 5. The joint PDF for the run A, in ''canonical'' variables X and Y, defined in Eq. (33). The two upper panels, (a) and (b), correspond to $r=1$, and the lower panels, (c) and (d), to $r=200$. The mesh surface presents the Gaussian joint PDF.

where $cr=3\sigma(r)$. Therefore, we will consider any contribution to the velocity increments beyond $3\sigma(r)$ as coming from the tails. That is, we define the contribution to the moments from the tails as

$$\langle u^m\rangle_t=\int_{-\infty}^{-cr}u^m p(u|r)du+\int_{cr}^{\infty}u^m p(u|r)du=\langle u^m\rangle-\langle u^m\rangle_c.$$

Figure 4(a) depicts $\sigma_2^2(r)=\langle u^2\rangle_c/\langle u^2\rangle$, corresponding to run A. We note first that, if the PDF is self-similar, then, by Eq. (16), $\sigma_2^2(r)=\langle u^2\rangle_c/\langle u^2\rangle=\int_{-3}^{3}\Phi(X)X^2dX$, and therefore it is independent of r. The figure shows, however, that this is not the case, and $\sigma_2(r)$ increases monotonously with r. As argued in [4], where this behavior of $\sigma_2(r)$ was also observed in the pipe turbulence, it happens because the contribution of the tails is more pronounced at small distances, and decreases with growing r. The growth of $\sigma_2(r)$ with distance showed some scaling, which was interpreted in [4] as a contribution to the inertial range coming from the tails. The scaling presented here corresponds to 1.5 decade. The scaling exponent almost coincides with corresponding exponent in [4] (which was 0.0028 ± 0.001), and this supports an assumption that intermittency (that is, in fact, a contribution from the tails) manifests itself in the inertial range (and not only in viscous scales).

The tails give an even more pronounced contribution to the higher moments, which is to be expected, of course. Figure 4(b) presents such a comparison for the third and the fifth order structure functions from run A. We took the odd structure functions because they do not vanish only due to asymmetry. In other words, the figure is intended to illustrate not so much the contribution of the tails compared with the contribution of the PDF core, but rather to illustrate the asymmetry of the tails. It can be seen indeed that the third moment is formed almost entirely by the tails, or rather, by their asymmetry. The cumulative part is small, and $\langle u^3\rangle_t$ is only slightly below the real moment $\langle u^3\rangle$. Moreover, the fitting for the tail part $\langle u^3\rangle_t\sim r^{0.979\pm0.008}$ is even slightly closer to the Kolmogorov law (42) than the fitting for the real moment, $\langle u^3\rangle\sim r^{1.039\pm0.003}$. The fittings are shown by bold straight lines, and the scaling holds for a decade and a half. For comparison, on the same figure, we also show the generalized structure function $\langle|u|^3\rangle$, and its tail part, $\langle|u|^3\rangle_t$. It can be seen that, unlike the third order structure function, the generalized structure function is noticeably higher than its tail part. Clearly, the third moment is not a high one, and therefore the tails do not give substantial contribution to it. The asymmetry of the tails, however, proves to contribute more to the third order structure function.

As to the fifth moment, the tails' contribution practically entirely defines it: the tail part is indistinguishable from $\langle u^5\rangle$

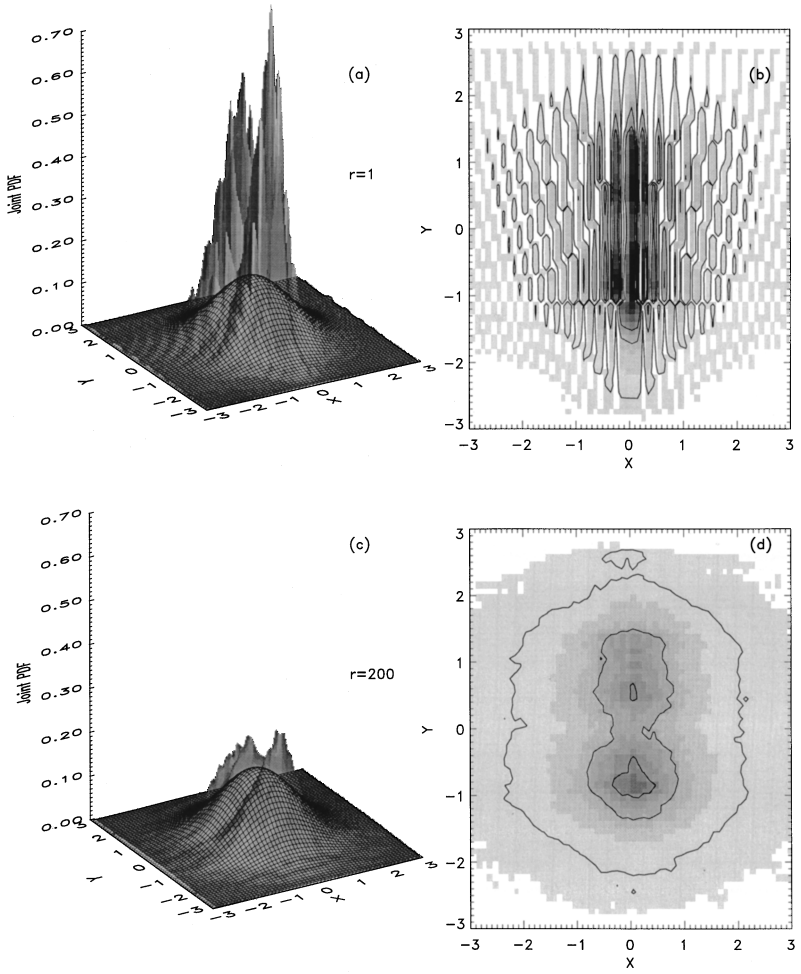

FIG. 6. The same as on Fig. 5, but for the run B.

in Fig. 4(b), the cumulative part giving a negligible contribution. Note one common trend on this figure: the contribution of the tails is always bigger at small distances, and decreases with growing r: that is, the tail part of the moments is always closer to the moment itself for small distances than it is for the large distances. This, of course, corresponds to the known fact that the tails are stronger at small r. It is noteworthy, however, that the tail contribution deviates noticeably for the generalized structure function of the third moment even for the smallest r's (increasing, of course, with r).

The contribution of the tails was checked in the same way with other runs. We constructed cumulative structure functions for the runs B, C, and D, to find qualitative agreement with Fig. 4. Namely, the Kolmogorov law is formed mostly by the tails, unlike the generalized structure function of the third order; and the fifth moment structure function is formed almost entirely by the tails.

VI. EXPERIMENTAL MEASUREMENTS OF THE TWO-POINT JOINT PDF

The measurements of the deviation from self-similarity (if any) for the two-point PDF is useful to provide in dimensionless variables (33). This form also easily reveals the asymmetry of the PDF. Figure 5 depicts this kind of PDF for the core, that is, when both arguments change within three standard deviations. This PDF is constructed for run A. We see that, first, the difference from a Gaussian distribution for small distances is really dramatic. It is a factor of 3 or 4. Second, for the big distances the PDF becomes quite close to Gaussian. In other words, the PDF changes substantially with r, and hence the PDF is not even nearly self-similar. The same two trends can be followed from Fig. 6, corresponding to run B. Furthermore, these trends definitely exist in all runs, not presented here in the figures.

These two figures, 5 and 6, reveal some puzzling features with symmetry. What one would expect is asymmetry in respect to X, that is, traditional asymmetry due to the Kolmogorov law, at least. It is clear, however, from Figs. 5(b) and 6(b) that the contours are quite symmetric with respect to the X axis. This may be explained by recalling that the asymmetry is only noticeable at the velocity increments PDF core (and it is quite pronounced at the tails, as seen, e.g., from Fig. 3). What is really surprising is that the joint PDF is rather asymmetric with respect to the Y axis, as seen from Figs. 5(b) and 6(b). This asymmetry is decreasing with growing distance r, and for big distances the PDF is more or less symmetric; see Figs. 5(d) and 6(d). The latter trend of decreasing asymmetry can be explained by decreasing statistical coherence between two points, when the distance is sufficiently big. For large distances, both variables X and Y

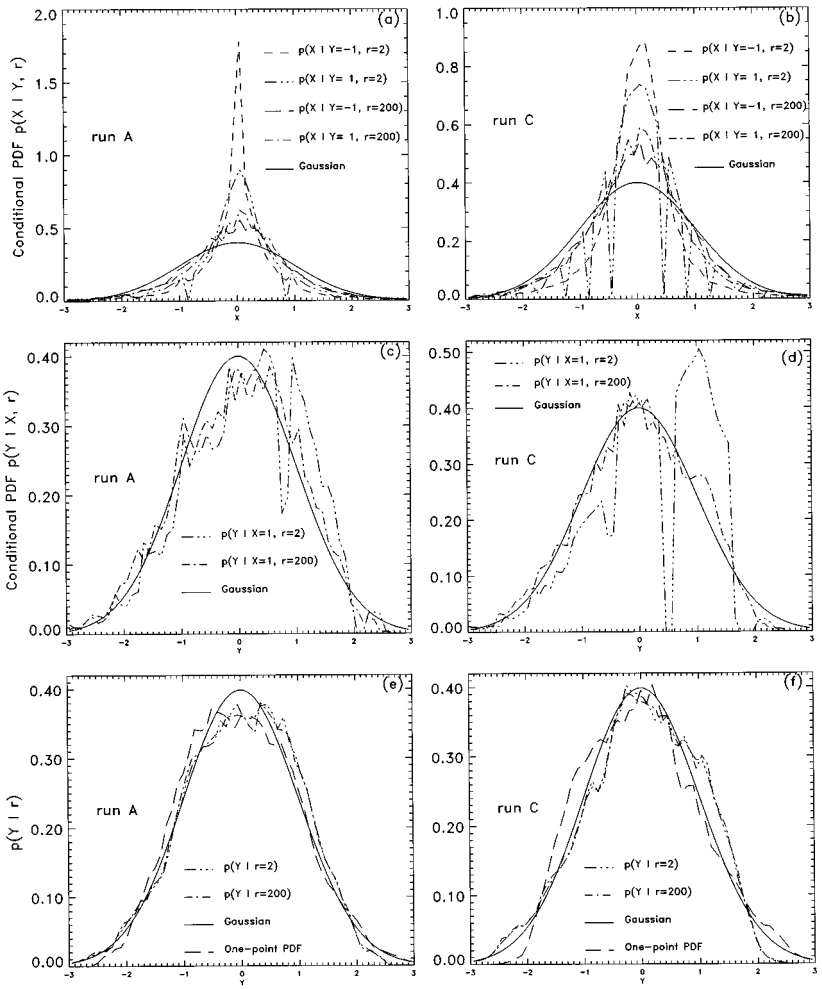

FIG. 7. Behavior and evolution of the PDF's with respect to the variable Y, for different distances r, and compared with Gaussian distribution (always depicted by a solid line). The left column [i.e., panels (a), (c), and (e)] corresponds to run A, and the right column [panels (b), (d), and (f)] corresponds to run C. The first row, (a) and (b), depicts conditional PDF as functions of the X variable, and for fixed $Y=\pm 1$. The distance is also fixed, and is presented by two values, $r=2$ and $r=200$. On the second row, (c) and (d), the conditional PDF is depicted as a function of Y, for $X=1$, and for the same distances $r=2$ and $r=200$. Finally, the third row, (e) and (f), depicts the PDF as a function of Y, for the same distances. They are compared with one-point PDF from the same runs.

present a sum of two statistically independent quantities, and therefore should not differ from each other in a statistical sense.

To follow this puzzling asymmetry, we constructed conditional PDF's involving Y dependence on Fig. 7. As seen from panel (a), the conditional PDF is still quite symmetric with respect to X. However, these two functions, $p(X|Y=1,r=2)$ and $p(X|Y=-1,r=2)$, being symmetric with respect to X, are quite different (by a factor of two); and both functions differ substantially from a Gaussian distribution. For big distances this disparity vanishes. The same trends are seen in Fig. 7(b), corresponding to run C, although the difference between $p(X|Y=1,r=2)$ and $p(X|Y=-1,r=2)$ is less pronounced.

The asymmetry with respect to Y can be seen directly from the Y dependence in Figs. 7(c) and 7(d), where conditional PDF $p(Y|X=1,r=2)$ and $p(Y|X=1,r=200)$ are depicted. The gravity centers of these curves are noticeably shifted to the right, and this time the asymmetry is more pronounced for run C, as compared with run A. Note that the mean velocity is subtracted from the data, so that $\langle v\rangle=0$, and therefore this shifting has nothing to do with the large scale velocity.

Finally, panels (e) and (f) of Fig. 7 depict the PDF $p(Y|r=2)$ and $p(Y|r=200)$, they are compared with Gaussians, and with one-point PDF $p(v/\langle v^2\rangle^{1/2})$ (where again $\langle v\rangle=0$). We notice a slight asymmetry with the same trend; i.e., the PDF's are shifted to the positive values, but only slightly. The most important feature, though, is the independence of the PDF from distance r. The PDF's show only very little difference when the distance increases. In fact, we measured the Y distribution PDF for bigger distances, up to $r=2000$, with wider range for the variable Y (up to $\pm 8\sigma'$), and the PDF's still look almost the same. We found no tails in the Y distribution, that is, unlike Fig. 3, the distribution goes to zero at $|Y|>3.5$, say, so that is goes even below the Gaussian distribution for large $|Y|$. This picture is repeated in all runs. All this suggests that the Y distribution *is* self-similar. Furthermore, as seen from these panels, there is not much difference between these PDF's and the Gaussian distribution on one hand, and with the one-point distribution on the other.

In summary, the PDF core, that is the distribution for moderate X and Y ($|X|,|Y|\leqslant 3$), is quite symmetric with respect to the X variable, but shows noticeable asymmetry with respect to the Y variable. Besides, the PDF is far from being self-similar. However, both asymmetry and non-self-similarity disappear if the PDF is integrated over X, that is, for pure Y distribution $p(Y|r)$.

VII. CONCLUSION

We see that asymmetry is tightly related to the deviation from self-similarity, and hence, it is related to intermittency. The asymmetry follows *a priori* from the Kolmogorov law (19): the third order structure function should vanish if the PDF is symmetric. Therefore, the PDF cannot coincide with Gaussian distribution *a priori*, the latter being the simplest and most natural self-similar distribution. Moreover, a self-similar PDF $p(X|r)$, X defined in Eq. (33a), is a function of X only. However, due to the asymmetry, the PDF should be written in the form (16), which is, strictly speaking, not self-similar, because it is a function of r as well.

These two deviations from self-similarity *a priori* are well known, and they were not expected to result in a drastic change of statistics. This is certainly true, at least because the deviation from self-similarity is a subtle effect, rather than dramatic. Nevertheless, a careful study of asymmetry proved to be useful, the latter being quite sensitive to the deviation. In particular, simple geometrical considerations, resulting in the ramp model [6], link the asymmetry with intermittency, as follows from expression (45). The measurements presented in this paper confirm this inequality; see Fig. 2(b).

Still, this effect is subtle. Indeed, as seen from Table I, the differences between plus and minus exponents are small, although they definitely are within the confidence level. The only exception is the Kolmogorov capacities for the plus and minus distributions; see inset to Fig. 1(a): the difference is appreciable. Of course, dealing with intermittency, we are implying in fact rare events: that is, we are implying that high fluctuations are happening much more often than what would follow from, say, a Gaussian distribution, but still rarely. Now, relating the intermittency with asymmetry means that the latter is manifested mainly in the tails of the distributions. Direct measurements of the tails show that they are asymmetric; see Fig. 3. Further, direct measurements of the contributions of the tails into the odd moments [results depicted on Fig. 4(b)] indicate that the tails give most of the contribution. These effects are not at all subtle.

Other substantial deviations from self-similarity are observed for the joint two-point PDF. First, it deviates quite substantially from the Gaussian distribution for relatively small distances r, even at the core of the distribution (see Figs. 5 and 6) quite unlike the classical PDF for the velocity increments: the latter, as mentioned, deviates from the Gaussian distribution on 10–15% (see, e.g., Fig. 5 of [4]). Second and more important is that the joint PDF is not at all self-similar. In addition, and quite unexpectedly, the joint PDF is asymmetric with respect to the Y coordinate, instead of being asymmetric with respect to the X axis.

This striking asymmetry with respect to the Y axis is a challenge yet to be explained. We can speculate that the Navier-Stokes equation is not symmetric with respect to $v\rightarrow -v$, and therefore not symmetric with respect to the $Y\rightarrow -Y$ transformation. Nevertheless, there are no known *a priori* reasons why the one-point distribution should be asymmetric. If it is symmetric, then it is easy to show that all odd moments $\langle Y^{2m+1}\rangle$ vanish (unlike the odd moments for the X distribution). That is to say that the Y PDF $p(Y|r)$ should be symmetric: and, according to Figs. 7(e) and 7(f), it is quite symmetric. On the other hand, the $Y\rightarrow -Y$ asymmetry of the Navier-Stokes equation appears due to the nonlinear term, or nonlinear interaction, and the same nonlinear interaction is also responsible for the nonvanishing third moment of the X distribution: see Eq. (19), i.e., the Kolmogorov law. This breaking of the symmetry due to nonlinearity, acting both on the X and the Y distribution, may be the reason why the joint PDF is asymmetric.

ACKNOWLEDGMENTS

The measurements of the atmospheric turbulence were made at Yale University, and were provided to me by K. R. Sreenivasan and B. Dhruva; I also appreciate discussions with them. I thank A. Yaglom for his interest in this paper, and for discussions.

[1] A. N. Kolmogorov, C. R. Acad. Sci. U.S.S.R. **32**, 16 (1941).
[2] A. N. Kolmogorov, C. R. Acad. Sci. U.S.S.R. **30**, 301 (1941).
[3] K. R. Sreenivasan, Annu. Rev. Fluid Mech. **29**, 435 (1997).
[4] S. I. Vainshtein, Phys. Rev. E **56**, 447 (1997).
[5] A. S. Monin and A. M. Yaglom, *Statistical Fluid Mechanics*, Vol. 2 (MIT Press, Cambridge, MA, 1971).
[6] S. I. Vainshtein and K. R. Sreenivasan, Phys. Rev. Lett. **73**, 3085 (1994).
[7] K. R. Sreenivasan, S. I. Vainshtein, R. Bhiladvala, I. San Gil, S. Chen, and N. Cao, Phys. Rev. Lett. **77**, 1488 (1996).
[8] According to the second Kolmogorov hypothesis, the PDF is uniquely determined by the quantity ϵ [2], or, the PDF for $u/(r\epsilon)^{1/3}$ should be universal [3]. The PDF in the form (16) with $\sigma(r)$ defined by Eq. (20) (which is a direct consequence of the Kolmogorov law) is indeed defined by the quantity ϵ, but *not uniquely*. In other words, the self-similarity requirement for the PDF (3), plus the Kolmogorov law result in expression (16) with *arbitrary* function Φ, that is, in slightly relaxed form of the second hypothesis. Note that universal function Φ would imply not only the scaling (21), (22) for all moments, but also the universality of *all* coefficients $\tilde{s}(m)$, $s(q)$, and C_2, in these expressions. That would be quite a strong restriction. In particular, it is known that the so-called Kolmogorov constant C, appearing as a coefficient of Fourier transform of the second order structure functions (21) and (22), and therefore unambiguously related to the coefficient C_2, is only approximately constant, see K. R. Sreenivasan, Phys. Fluids **7**, 2778 (1995). Direct measurements of this function also show that it is not universal, and in fact it is different for

different distances, see [4], and Sec. V of this paper for more details.

[9] F. Anselmet, Y. Gagne, E. J. Hopfinger, and R. A. Antonia, J. Fluid Mech. **140**, 63 (1984); R. Benzi, L. Biferale, S. Ciliberto, R. Tripiccione, C. Baudet, F. Massaioli, and S. Succi, Phys. Rev. E **48**, R30 (1993); G. Stolovitzky, K. R. Sreenivasan, and A. Juneja, *ibid.* **48**, R3217 (1993); L. Zubair, Ph.D. thesis, Yale University, 1993; C. Meneveau and K. R. Sreenivasan, Nucl. Phys. B (Proc. Suppl.) **2**, 49 (1987); R. R. Prasad, C. Meneveau, and K. R. Sreenivasan, Phys. Rev. Lett. **61**, 74 (1988); C. Meneveau, K. R. Sreenivasan, P. Kailasnath, and M. S. Fan, Phys. Rev. A **40**, 894 (1989); E. Aurell, U. Frisch, J. Lutsko, and M. Vergassola, J. Fluid Mech. **238**, 467 (1992); M. Borgas, Philos. Trans. R. Soc. London Ser. A **342**, 379 (1993).

[10] P. Kailasnath, K. R. Sreenivasan, and G. Stolovitzky, Phys. Rev. Lett. **68**, 2766 (1992).

[11] B. Castaing, Y. Gagne, and E. J. Hopfinger, Physica D **46**, 177 (1990); R. Benzi, L. Biferale, G. Paladin, A. Vulpiani, and M. Vergassola, Phys. Rev. Lett. **67**, 2299 (1991); P. Tabeling, G. Zocchi, F. Belin, J. Maurer, and H. Willaime, Phys. Rev. E **53**, 1613 (1996); A. Noullez, G. Wallace, W. Lempert, R. B. Miles, and U. Frisch, J. Fluid Mech. **339**, 287 (1997).

[12] C. Meneveau and K. R. Sreenivasan, J. Fluid Mech. **224**, 429 (1991).

[13] A. N. Kolmogorov, J. Fluid Mech. **13**, 82 (1962).

[14] S. I. Vainshtein, K. R. Sreenivasan, R. T. Pierrehumbert, V. Kashyap, and A. Juneja, Phys. Rev. E **50**, 1823 (1994).

[15] H. G. E. Hentschel and I. Procaccia, Physica D **8**, 435 (1983); U. Frisch and G. Parisi, in *Turbulence and Predictability in Geophysical Fluid Dynamics*, edited by M. Gil, R. Benzi, and G. Parisi (North-Holland, Amsterdam, 1985), pp. 84–88; G. Paladin and A. Vulpiani, Phys. Rep. **156**, 147 (1987).

[16] N. Cao, S. Chen, and K. R. Sreenivasan, Phys. Rev. Lett. **77**, 3799 (1996).